Electronic Supplementary Material (ESI) for Organic & Biomolecular Chemistry.
This journal is © The Royal Society of Chemistry 2017

Supporting information

Forsythenethosides A and B: Two New Phenylethanoid Glycosides with a 15-Membered Ring from *Forsythia suspensa*

Si-Yuan Shao, Zi-Ming Feng, Ya-Nan Yang, Jian-Shuang Jiang, and Pei-Cheng Zhang*

State Key Laboratory of Bioactive Substance and Function of Natural Medicines, Institute of Materia Medica, Chinese Academy of Medical Sciences and Peking Union Medical College, Beijing 100050, People's Republic of China

no.	content	page
1	Experimental section	S3
2	**Table S1.** Energies of dominant conformers of **1a** and **1b** at B3LYP/6-31+G(d,p) in DMSO	S4
3	**Table S2.** Weighted average distances and standard deviations calculated upon dominant conformers for **1a** and **1b**	S5
4	**Figure S1.** GC analysis of derivatives of D-glucose, L-glucose, D-xylose, L-xylose and hydrolysates of **1**	S6
5	**Table S3.** Neuroprotective activities of extracts against rotenone-induced PC12 cell damage	S7
6	**Table S4.** Neuroprotective activities of **1** and **2** against serum-deprivation-induced PC12 cell damage and rotenone-induced PC12 cell damage	S8
7	**Figure S2.** UV spectrum of **1**	S9
8	**Figure S3.** IR spectrum of **1**	S10
9	**Figure S4.** HRESIMS of **1**	S11
10	**Figure S5.** ^{1}H NMR spectrum of **1** in DMSO-d_6 (500 MHz)	S12
11	**Figure S6.** ^{13}C NMR spectrum of **1** in DMSO-d_6 (125 MHz)	S13
12	**Figure S7.** DEPT NMR spectrum of **1** in DMSO-d_6 (125 MHz)	S14
13	**Figure S8.** HSQC spectrum of **1** in DMSO-d_6 (500 MHz)	S15
14	**Figure S9.** HMBC spectrum of **1** in DMSO-d_6 (500 MHz)	S16
15	**Figure S10.** ^{1}H-^{1}H COSY spectrum of **1** in DMSO-d_6 (500 MHz)	S17
16	**Figure S11.** TOCSY spectrum of **1** in DMSO-d_6 (500 MHz)	S18
17	**Figure S12.** ROESY spectrum of **1** in DMSO-d_6 (500 MHz)	S19
18	**Figure S12a.** Expanded ROESY spectrum of **1** in DMSO-d_6 (500 MHz)	S20
19	**Figure S13.** UV spectrum of **2**	S21
20	**Figure S14.** IR spectrum of **2**	S22
21	**Figure S15.** HRESIMS of **2**	S23
22	**Figure S16.** ^{1}H NMR spectrum of **2** in DMSO-d_6 (500 MHz)	S24

23	**Figure S17.** ^{13}C NMR spectrum of **2** in DMSO-d_6 (125 MHz)	S25
24	**Figure S18.** DEPT NMR spectrum of **2** in DMSO-d_6 (125 MHz)	S26
25	**Figure S19.** HSQC spectrum of **2** in DMSO-d_6 (500 MHz)	S27
26	**Figure S20.** HMBC spectrum of **2** in DMSO-d_6 (500 MHz)	S28
27	**Figure S21.** ^{1}H-^{1}H COSY spectrum of **2** in DMSO-d_6 (500 MHz)	S29
28	**Figure S22.** TOCSY spectrum of **2** in DMSO-d_6 (500 MHz)	S30
29	**Figure S23.** ROESY spectrum of **2** in DMSO-d_6 (500 MHz)	S31
30	**Figure S23a.** Expanded ROESY spectrum of **2** in DMSO-d_6 (500 MHz)	S32

Experimental section

Quantum Chemistry Calculation

Conformational analysis was initially performed using Discovery Studio (version 2016) at CHARMm force field for **1a** and **1b**. Energy cutoff was 20.0 kcal/mol and the maximum number of conformers was set 255 by default.

The theoretical calculation of conformers were carried out using Gaussian 09 program (Gaussian Inc., Wallingford, CT, USA).[1] The geometries of isomers were first optimized at HF/6-31G(d) in gas phase, and further optimized at B3LYP/6-31+G(d,p) using the polarizable continuum model (PCM) to take into account the solvent effect of DMSO. Vibrational frequency analysis was conducted to ensure that geometry optimizations had reached local minima. In order to reduce the high computational cost, room-temperature equilibrium populations for conformers after gas optimization were calculated according to Boltzmann distribution law (eq.1) and conformers with lower than 1% proportion were filtered.

$$\frac{N_i}{N} = \frac{g_i e^{-\frac{E_i}{k_B T}}}{\sum g_i e^{-\frac{E_i}{k_B T}}} \quad \textbf{(1)}$$

where N_i is the number of conformer i with energy E_i and degeneracy g_i at temperature T, and k_B is Boltzmann constant.

Finally, distances between hydrogen atoms were measured and weighted averages and standard deviations calculated according to Boltzmann-population.

Table S1. Energies of Dominant Conformers of 1a and 1b at B3LYP/6-31+G(d,p) in DMSO

stereoisomer	no.	conformer	E (Hartree)	E (kcal/mol)	population (%)
1a	1	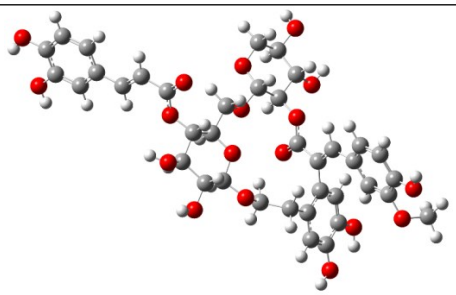	-2809.98412171	-1763291.64	98.35
	2	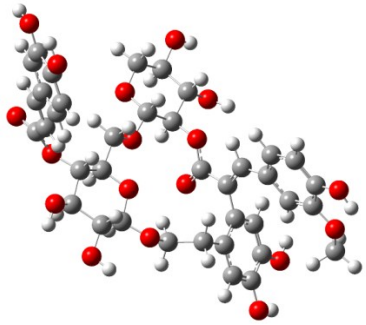	-2809.98000942	-1763289.06	1.26
	3	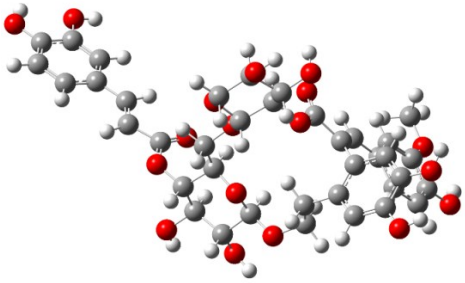	-2809.97870616	-1763288.25	0.32
1b	1	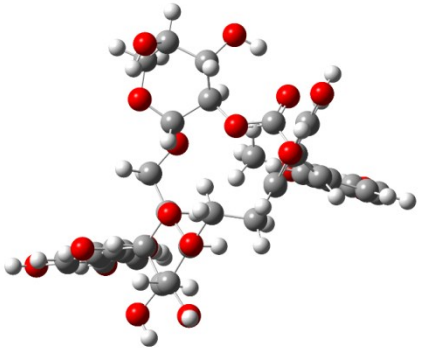	-2809.96638186	-1763280.51	15.01
	2	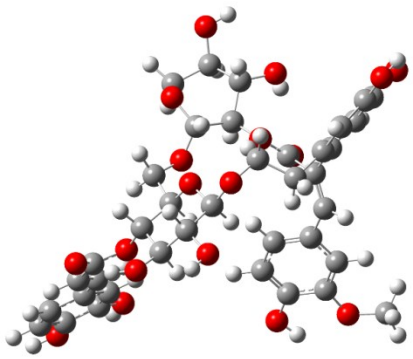	-2809.96801806	-1763281.54	84.99

Table S2. Weighted Average Distances and Standard Deviations Calculated upon Dominant Conformers for 1a and 1b

stereoisomer	conformer	distance (Å)			population (%)	predominant
		H-15/H-22	H-16/H-22	H-17/H-22		
1a	1	3.65	4.28	3.62	98.35	YES
	2	3.63	4.27	3.67	1.26	NO
	3	5.88	4.52	6.23	0.32	NO
	weighted average	3.66 ± 0.02	4.28 ± 0.00	3.63 ± 0.02		
1b	1	6.15	5.79	6.29	15.01	NO
	2	6.19	5.77	6.76	84.99	YES
	weighted average	6.18 ± 0.00	5.77 ± 0.03	6.69 ± 0.03		

Determination of the absolute configuration of sugars

Compound **1** (4 mg) was dissolved in 1M HCl (3 mL) to incubate at 65 °C for 14 h. After that, the reaction was concentrated to yield a residue. Then, the residue was suspended in water and then extracted with ethyl acetate (2 mL x 3). The water soluble layer was evaporated under vacuum and then dissolved in pyridine (2 mL). L-Cysteine methyl ester hydrochloride (2 mg) was added subsequently, and the reaction was maintained at 65 °C for 2 h. Then, *N*-trimethylsilylimidazole (0.6 mL) was added after the reaction was evaporated under vacuum. The reaction mixture was incubated at 65 °C for 2 h and partitioned between water and *n*-hexane (2 mL each for three times). Finally, the *n*-hexane layer was detected by GC experiment under the following conditions: capillary column, HP-5 (60 m × 0.25 mm, 0.25 μm, Dikma); detector, FID; detection temperature, 300 °C; injection temperature, 300 °C; initial temperature, 200 °C; raised to 260 °C at a rate of 10 °C/min, and maintained for 30 min, then declined to 200 °C at a rate of 40 °C/min and the temperature was maintained for 1 min; carrier, N_2 gas. D-glucose and D-xylose were determined by comparing their retention time with those of the authentic sugars, which displayed retention times of 29.5 and 19.0 min, respectively (Figure S1).

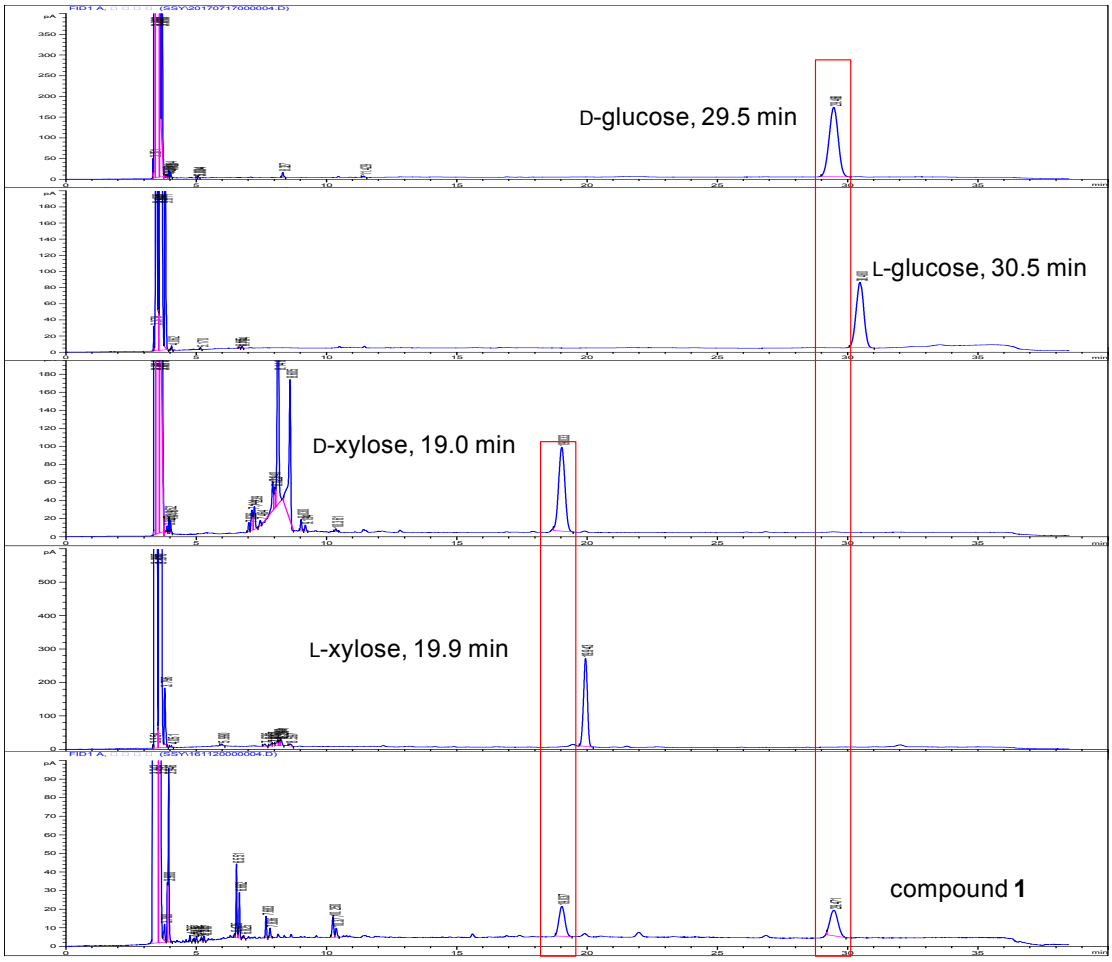

Figure S1. GC analysis of derivatives of D-glucose, L-glucose, D-xylose, L-xylose and hydrolysates of **1**.

Neuroprotective activities of extracts

The extracts of the fruits of *Forsythia suspensa* were tested for neuroprotective activities against rotenone-induced PC12 cell damage with an MTT assay (Table S3). The PC12 cells were cultured in Dulbecco's modified Eagle's medium supplemented (DMEM) with 5% horse serum and 5% fetal bovine serum. Then, 100 μL cells with an initial density of 5×10^4 cells/mL were seeded in each well of a poly-L-lysine-coated, 96-well culture plate and precultured for 24 h at 37 °C under a 5% CO_2 atmosphere. The medium was then replaced by different fresh medium including the control (complete medium), the model (complete medium with 4 μM rotenone), and the sample (complete medium with 4 μM rotenone and 10 μg/mL test samples), and the cells were cultured for 48 h. Then, 10 μL of MTT (0.5 mg/mL) was added to each well and maintained for 4 h, and then the medium was removed. The formazan crystals were dissolved in 100 μL DMSO and absorbance was measured on a microplate reader at 550 nm.[2] The cell viability (%) of each example was evaluated (Table S3).

Table S3. Neuroprotective Activities of Extracts against Rotenone-Induced PC12 Cell Damage (10 μg/mL means ± SD, n = 6)[a]

	rotenone (%)
group	10 μg/mL
control	100.0 ± 6.3
model	54.2 ± 2.8$^{\#\#\#}$
total extract	58.0 ± 4.4
petroleum ether fraction	54.0 ± 5.1
EtOAc fraction	56.0 ± 3.8
n-BuOH fraction	78.5 ± 5.0***
H_2O fraction	77.5 ± 2.6***

[a]$^{\#\#\#}p < 0.001$ vs. control, $^{***}p < 0.001$ vs. model.

Neuroprotective activities of 1 and 2

Rotenone-induced PC12 cell damage. Forsythenethosides A and B were tested for neuroprotective activities against rotenone-induced PC12 cell damage with an MTT assay (Table S4). The cells were cultured in Dulbecco's modified Eagle's medium supplemented (DMEM) with 5% horse serum and 5% fetal bovine serum. Then, 100 μL cells with an initial density of 5 × 10^4 cells/mL were seeded in each well of a poly-L-lysine-coated, 96-well culture plate and cultured for 24 h at 37 °C under a 5% CO_2 atmosphere. The medium was then replaced by different fresh medium including the control (complete medium), the model (complete medium with 4 μM rotenone), the positive contrast (complete medium with 4 μM rotenone and 50 ng/mL nerve growth factor), and the sample (complete medium with 4 μM rotenone and 10 μM test compounds), and cultured for 48 h. Then, 10 μL of MTT (0.5 mg/mL) was added to each well and maintained for 4 h before removing the medium. The formazan crystals were dissolved in 100 μL DMSO and absorbance was measured on a microplate reader at 550 nm. The cell viability (%) of each example was evaluated (Table S4).

Serum-deprivation-induced PC12 cell damage. Forsythenethosides A and B were tested for neuroprotective activities against serum-deprivation-induced PC12 cell damage with an MTT assay (Table S4). The PC12 cells were cultured in Dulbecco's modified Eagle's medium (DMEM) supplemented with 5% horse serum and 5% fetal bovine serum. Then, 100 μL cells with an initial density of 5 × 10^4 cells/mL were seeded in each well of a poly-L-lysine-coated, 96-well culture plate and cultured for 24 h at 37 °C under a 5% CO_2 atmosphere. The medium was then replaced by different fresh medium including the control (complete medium), the model (medium without serum), the positive contrast (medium without serum and 50 ng/mL nerve growth factor), and the sample (medium without serum and 10 μM test samples). Then, the cells were cultured in DMEM without serum for 48 h. Then, 10 μL of MTT (0.5 mg/mL) was added and maintained for 4 h before removing the medium. The formazan crystals were dissolved in 100 μL DMSO and

absorbance was measured on a microplate reader at 550 nm. The cell viability (%) of each example was evaluated (Table S4).

Table S4. Neuroprotective Activities of 1 and 2 against Serum-Deprivation-Induced PC12 Cell Damage and Rotenone-Induced PC12 Cell Damage (10 μM means ± SD, n = 12)[a]

	serum-deprivation (%)	rotenone (%)
group	10 μM	10 μM
control	100.0 ± 4.1	100.0 ± 3.0
model	31.3 ± 5.3$^{\#\#\#}$	59.9 ± 3.0$^{\#\#\#}$
NGF[b]	35.3 ± 4.7***	96.7 ± 3.1***
1	41.0 ± 4.9***	76.8 ± 2.3***
2	43.2 ± 5.7***	75.1 ± 3.8***

[a]$^{\#\#\#}p < 0.001$ vs. control, $^{***}p < 0.001$ vs. model. [b]NFG is the abbreviation of nerve growth factor.

Reference

(1) Frisch, M. J.; Trucks, G. W.; Schlegel, H. B.; Scuseria, G. E.; Robb, M. A.; Cheeseman, J. R.; Scalmani, G.; Barone, V.; Mennucci, B.; Petersson, G. A.; Nakatsuji, H.; Caricato, M.; Li, X.; Hratchian, H. P.; Izmaylov, A. F.; Bloino, J.; Zheng, G.; Sonnenberg, J. L.; Hada, M.; Ehara, M.; Toyota, K.; Fukuda, R.; Hasegawa, J.; Ishida, M.; Nakajima, T.; Honda, Y.; Kitao, O.; Nakai, H.; Vreven, T.; Montgomery, Jr., J. A.; Peralta, J. E.; Ogliaro, F.; Bearpark, M.; Heyd, J. J.; Brothers, E.; Kudin, K. N.; Staroverov, V. N.; Kobayashi, R.; Normand, J.; Raghavachari, K.; Rendell, A.; Burant, J. C.; Iyengar, S. S.; Tomasi, J.; Cossi, M.; Rega, N.; Millam, J. M.; Klene, M.; Knox, J. E.; Cross, J. B.; Bakken, V.; Adamo, C.; Jaramillo, J.; Gomperts, R.; Stratmann, R. E.; Yazyev, O.; Austin, A. J.; Cammi, R.; Pomelli, C.; Ochterski, J. W.; Martin, R. L.; Morokuma, K.; Zakrzewski, V. G.; Voth, G. A.; Salvador, P.; Dannenberg, J. J.; Dapprich, S.; Daniels, A. D.; Farkas, Ö.; Foresman, J. B.; Ortiz, J. V.; Cioslowski, J.; Fox, D. J. Gaussian 09, Rev. C 01; Gaussian, Inc., Wallingford CT, 2009.

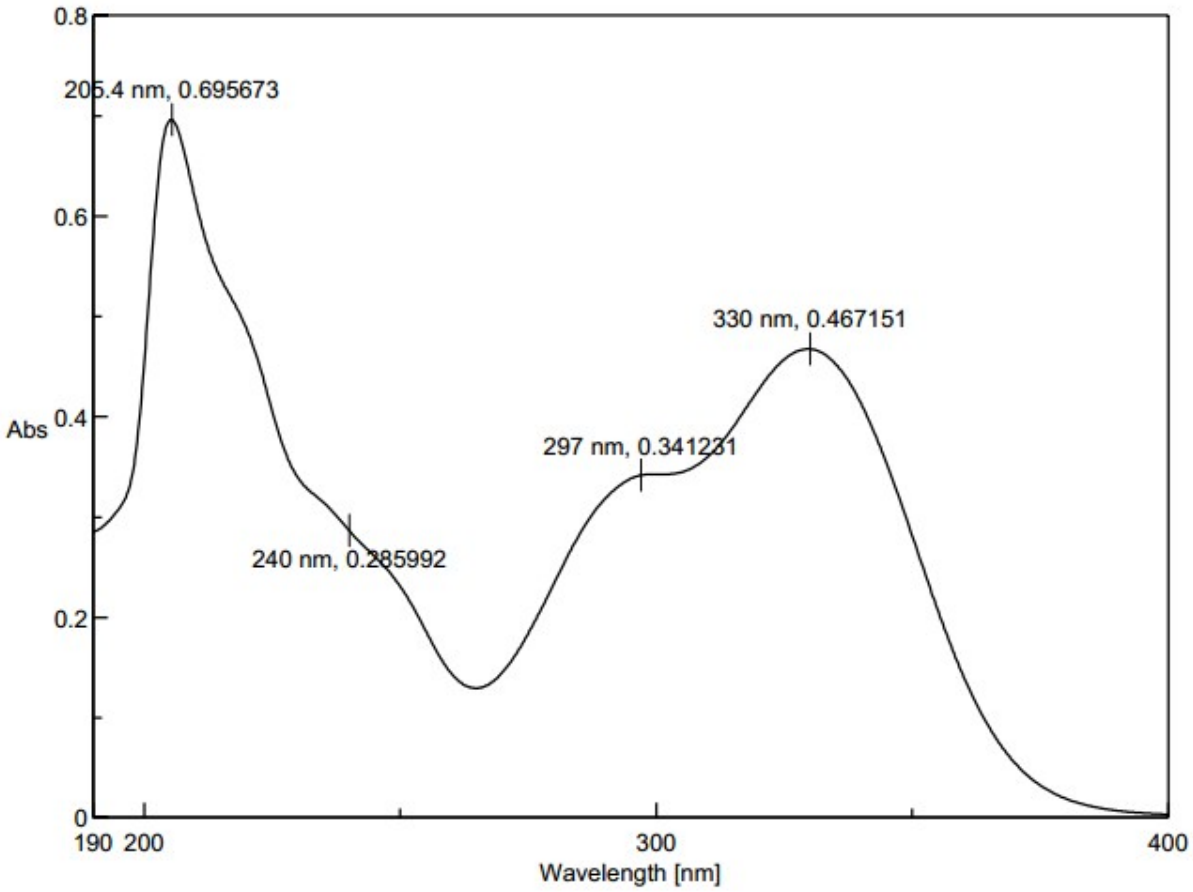

Figure S2. UV spectrum of **1**.

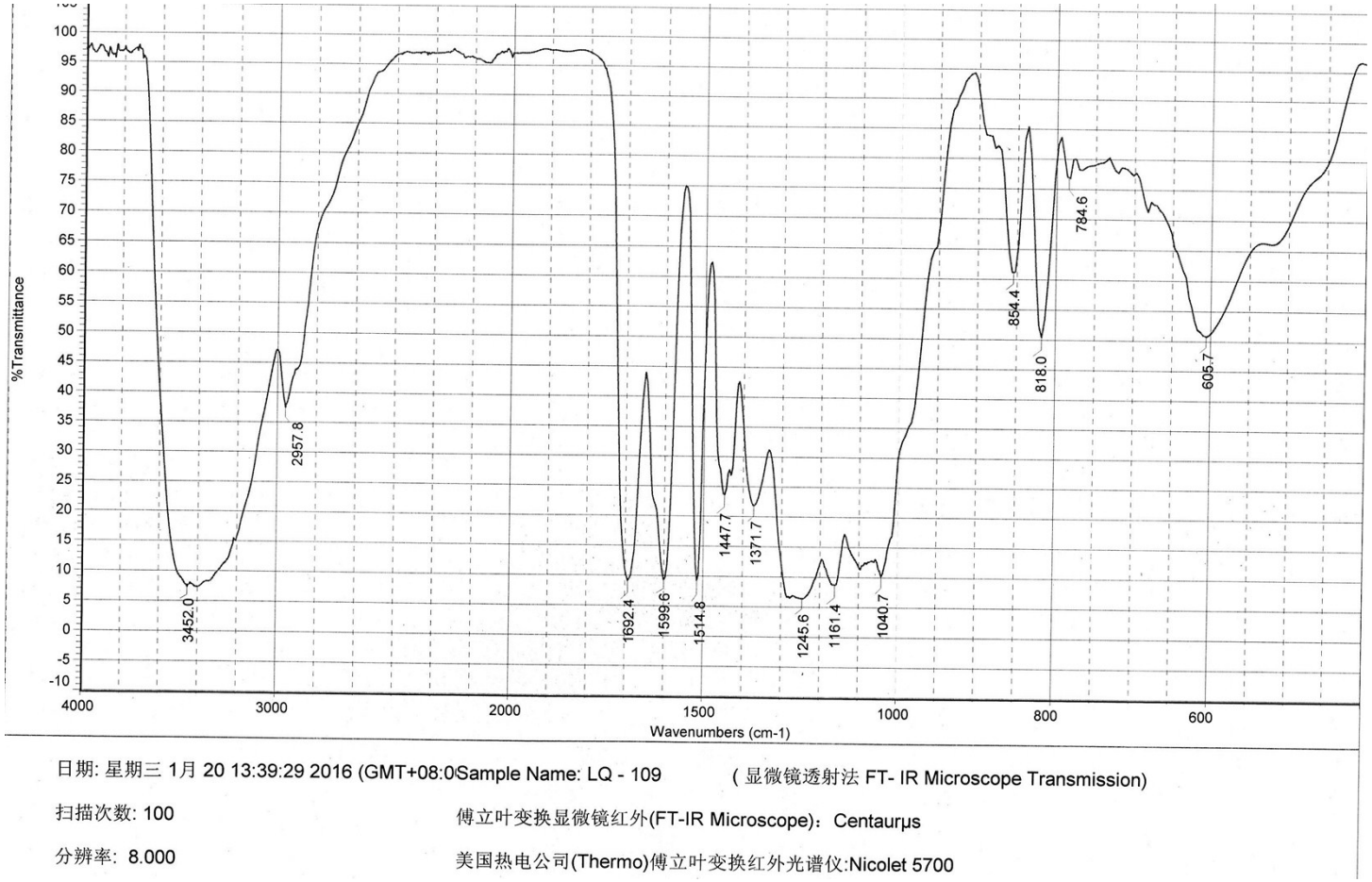

Figure S3. IR spectrum of **1**.

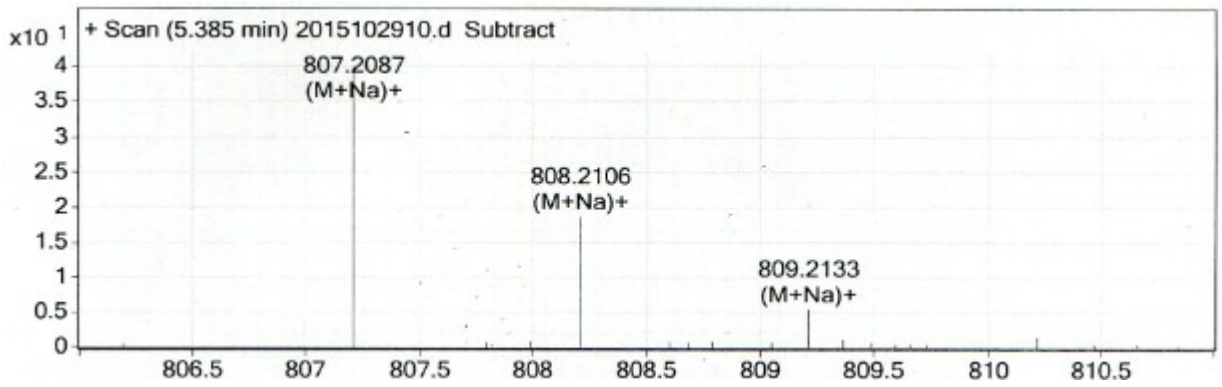

m/z	Ion	Formula	Abundance
807.20872	(M+Na)+	C38 H40 Na O18	51565.3

Best	Formula (M)	Ion Formula	Calc m/z	Score	Cross Score	Mass	Calc Mass	Diff (ppm)	Abs Diff (ppm)	Abund Match	Spacing Match	Mass Match	m/z
☑	C38 H40 O18	C38 H40 Na O18	807.21069	99.64		784.21936	784.22146	2.69	2.69	99.26	99.86	99.75	807.20872
☐	C39 H36 N4 O14	C39 H36 N4 Na O14	807.21202	99.59		784.21938	784.2228	4.37	4.37	99.73	99.89	99.35	807.20872
☐	C43 H36 N4 O9 S	C43 H36 N4 Na O9 S	807.20952	99.51		784.21939	784.2203	1.16	1.16	98.44	99.91	99.95	807.20872
☐	C42 H40 O13 S	C42 H40 Na O13 S	807.20818	99.5		784.21937	784.21896	-0.52	0.52	98.34	99.89	99.99	807.20872
☐	C45 H36 O13	C45 H36 Na O13	807.20481	99.41		784.21936	784.21559	-4.8	4.8	99.38	99.84	99.21	807.20872
☐	C46 H32 N4 O9	C46 H32 N4 Na O9	807.20615	99.39		784.21938	784.21693	-3.12	3.12	98.54	99.88	99.67	807.20872
☐	C33 H40 N2 O20	C33 H40 N2 Na O20	807.20666	98.95		784.21937	784.21744	-2.46	2.46	96.77	99.89	99.79	807.20872
☐	C51 H32 N2 O7	C51 H32 N2 Na O7	807.21017	98.84		784.21937	784.22095	2.02	2.02	96.29	99.85	99.86	807.20872
☐	C37 H40 N2 O15 S	C37 H40 N2 Na O15 S	807.20416	98.8		784.21938	784.21494	-5.66	5.66	97.73	99.88	98.91	807.20872
☐	C47 H36 N4 O4 S2	C47 H36 N4 Na O4 S2	807.20702	98.08		784.21939	784.2178	-2.04	2.04	93.66	99.83	99.86	807.20872

Figure S4. HRESIMS of **1**.

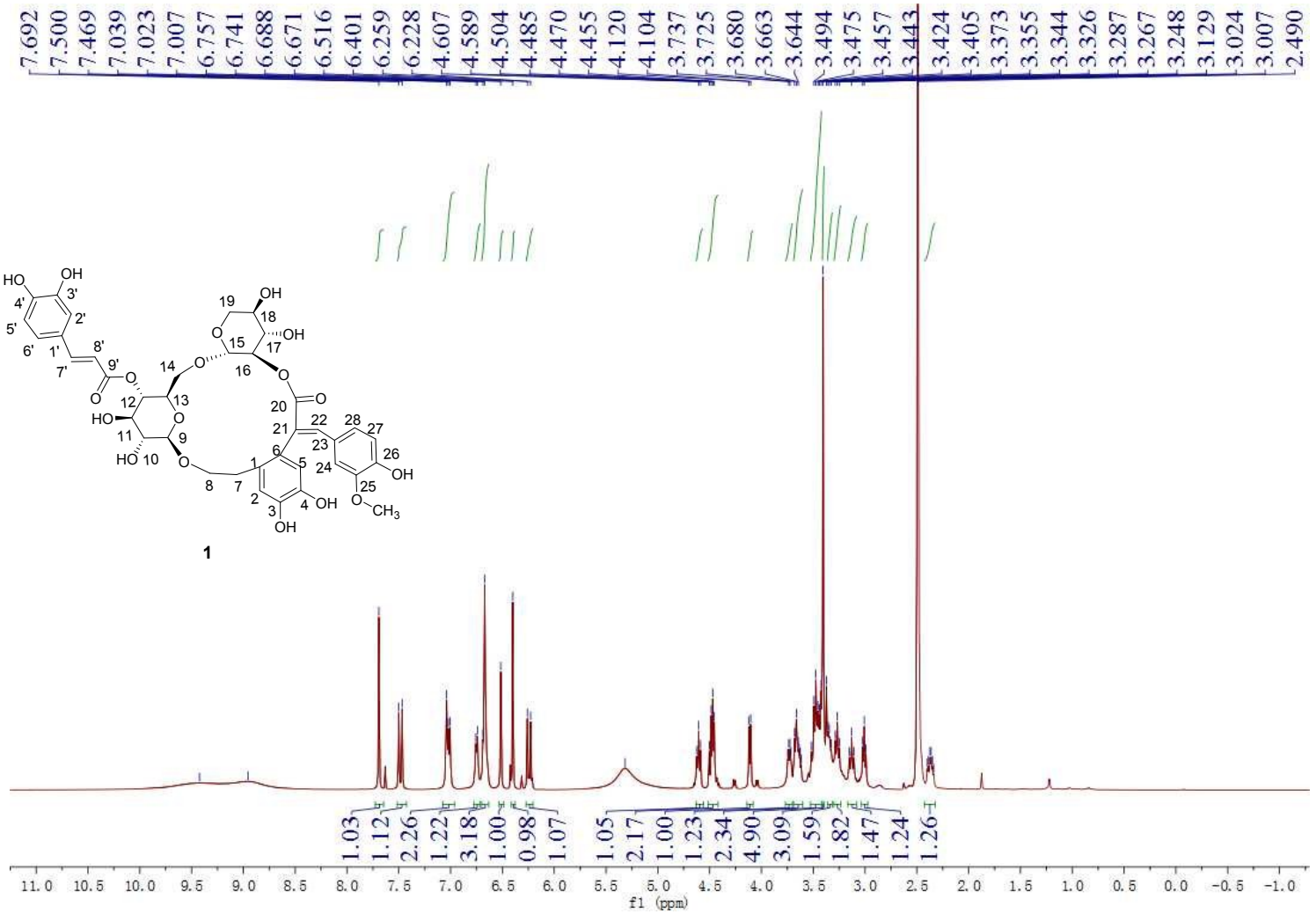

1

Figure S5. ^{1}H NMR spectrum of **1** in DMSO-d_6 (500 MHz).

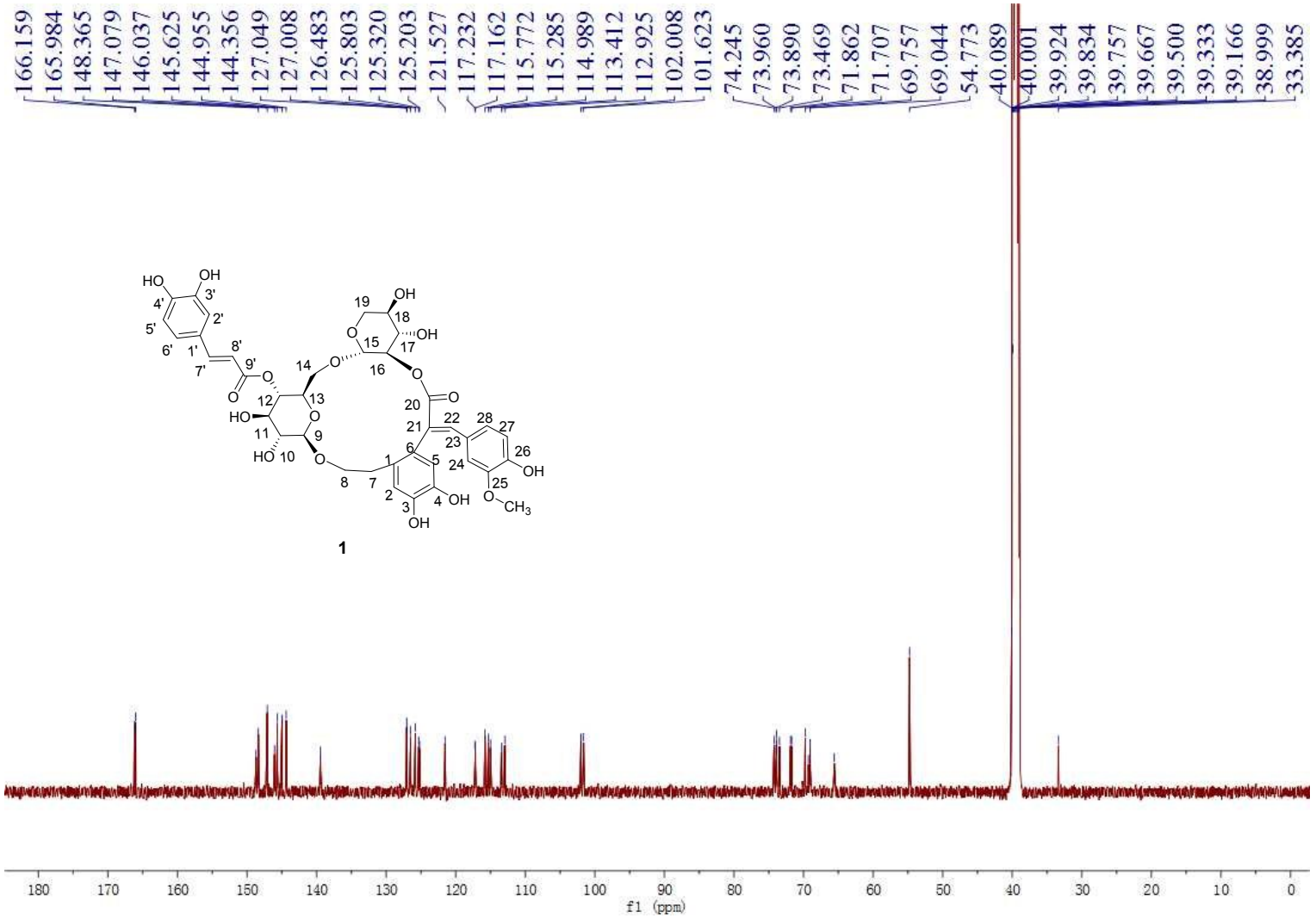

Figure S6. ^{13}C NMR spectrum of **1** in DMSO-d_6 (125 MHz).

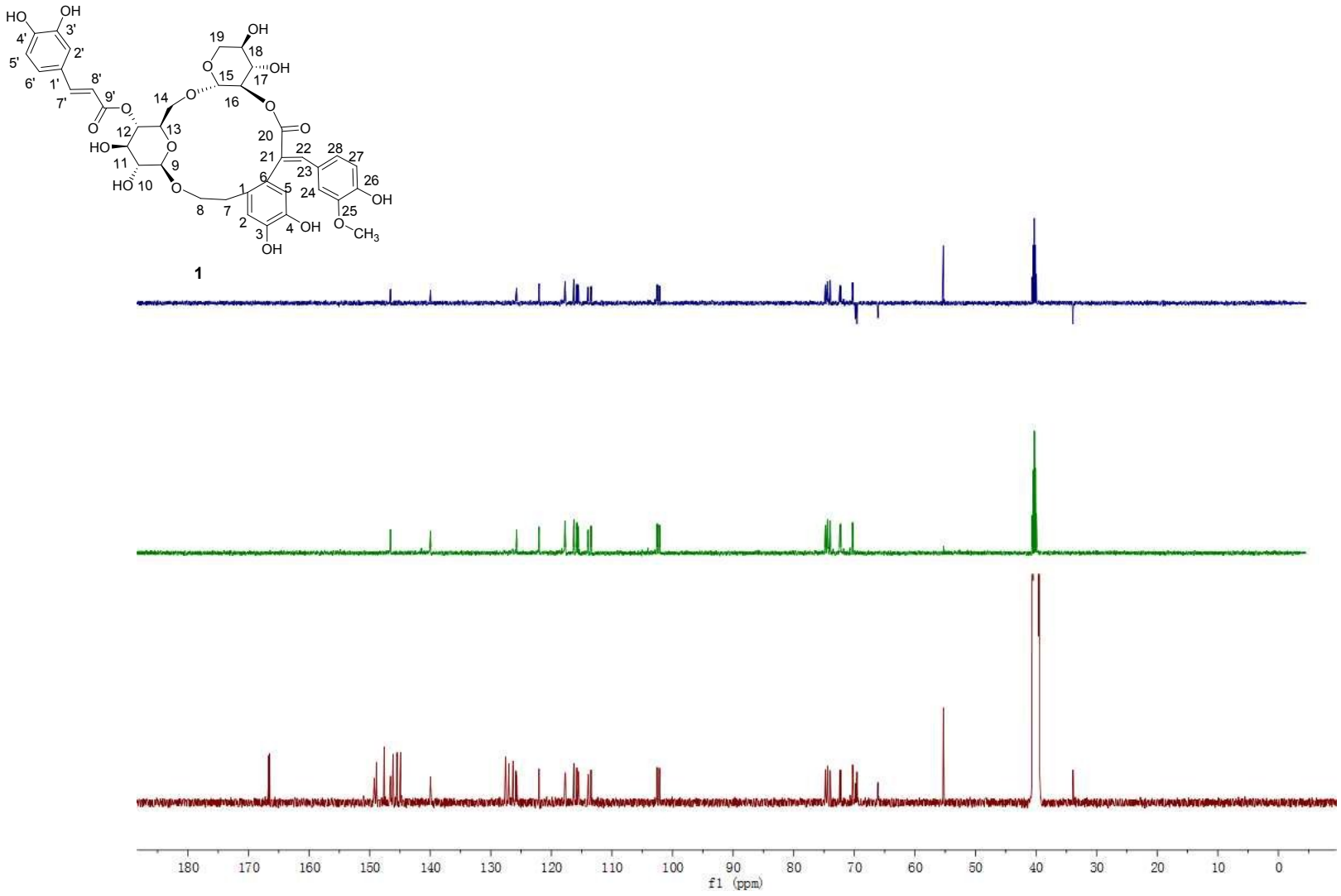

Figure S7. DEPT NMR spectrum of **1** in DMSO-d_6 (125 MHz).

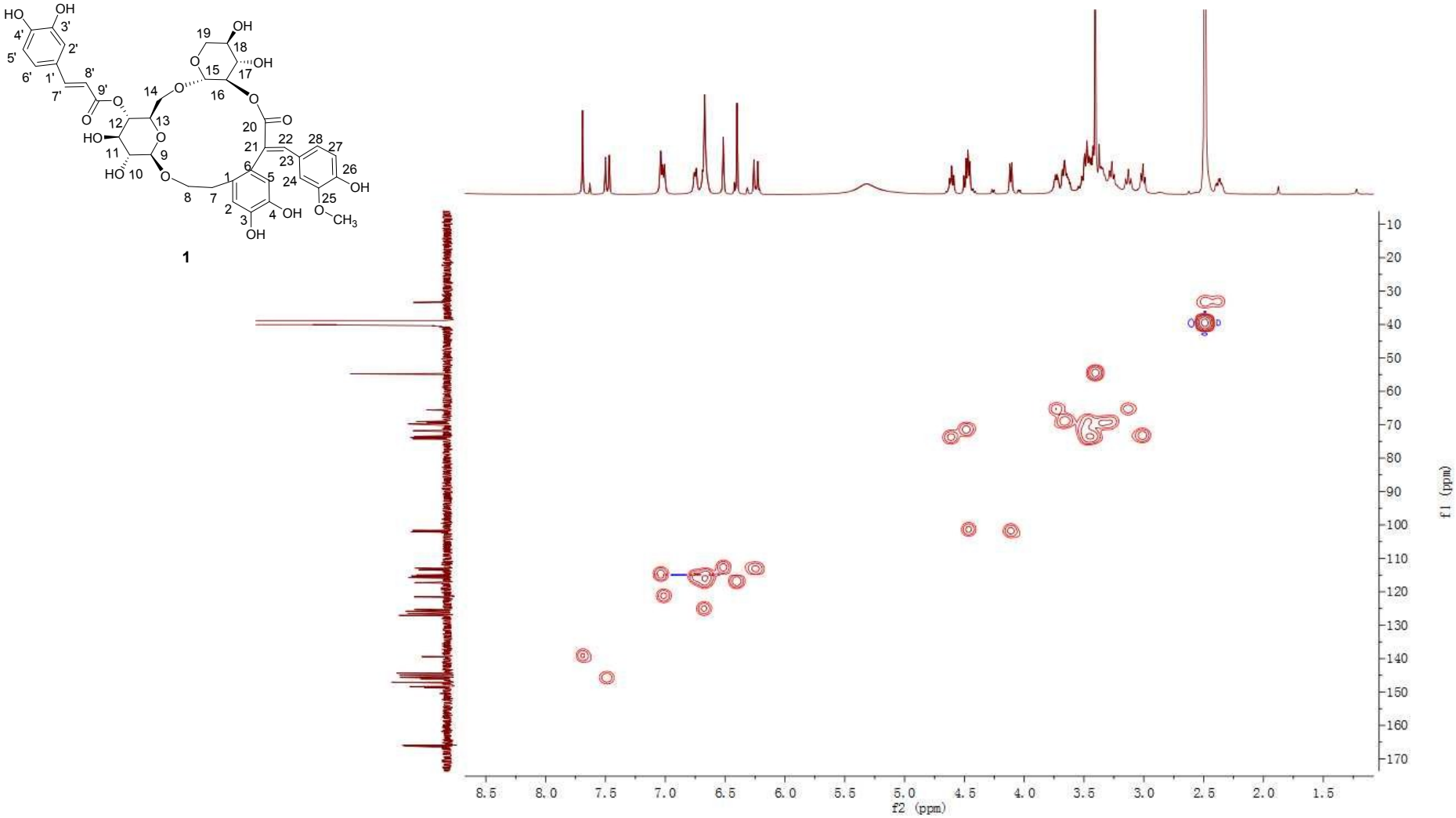

Figure S8. HSQC spectrum of **1** in DMSO-d_6 (500 MHz).

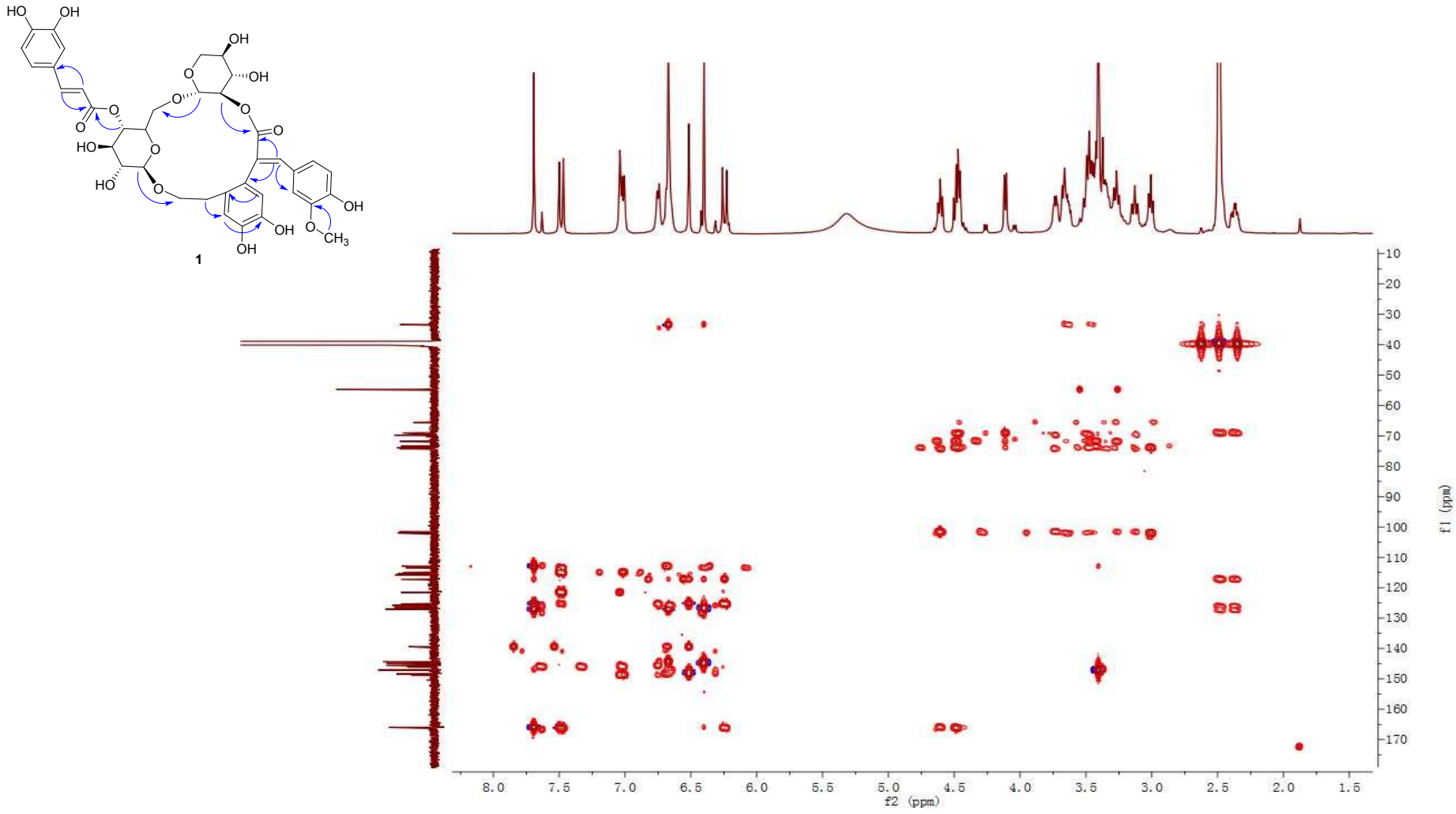

Figure S9. HMBC spectrum of **1** in DMSO-d_6 (500 MHz).

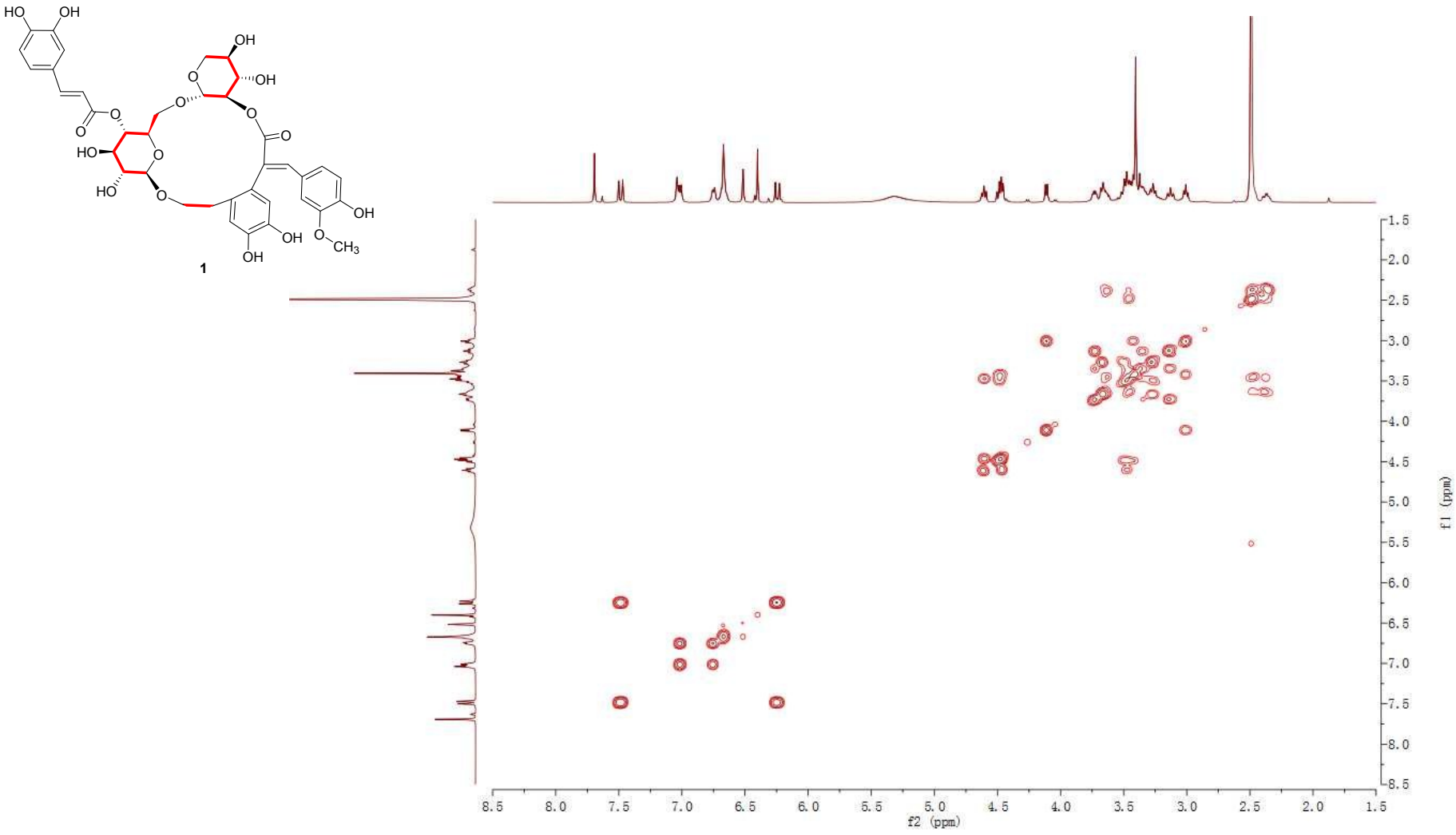

Figure S10. ^{1}H-^{1}H COSY spectrum of **1** in DMSO-d_6 (500 MHz).

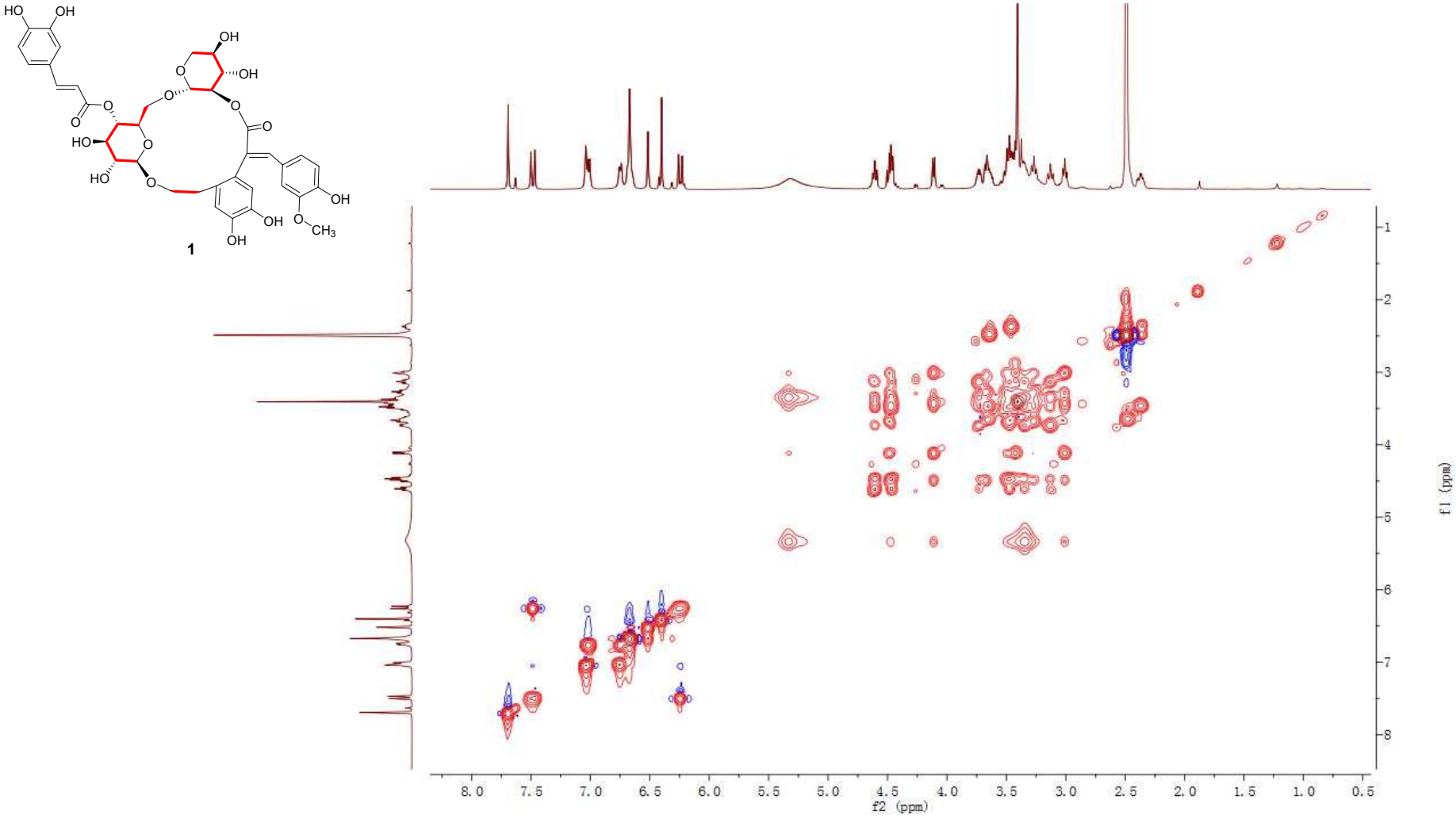

Figure S11. TOCSY spectrum of **1** in DMSO-d_6 (500 MHz).

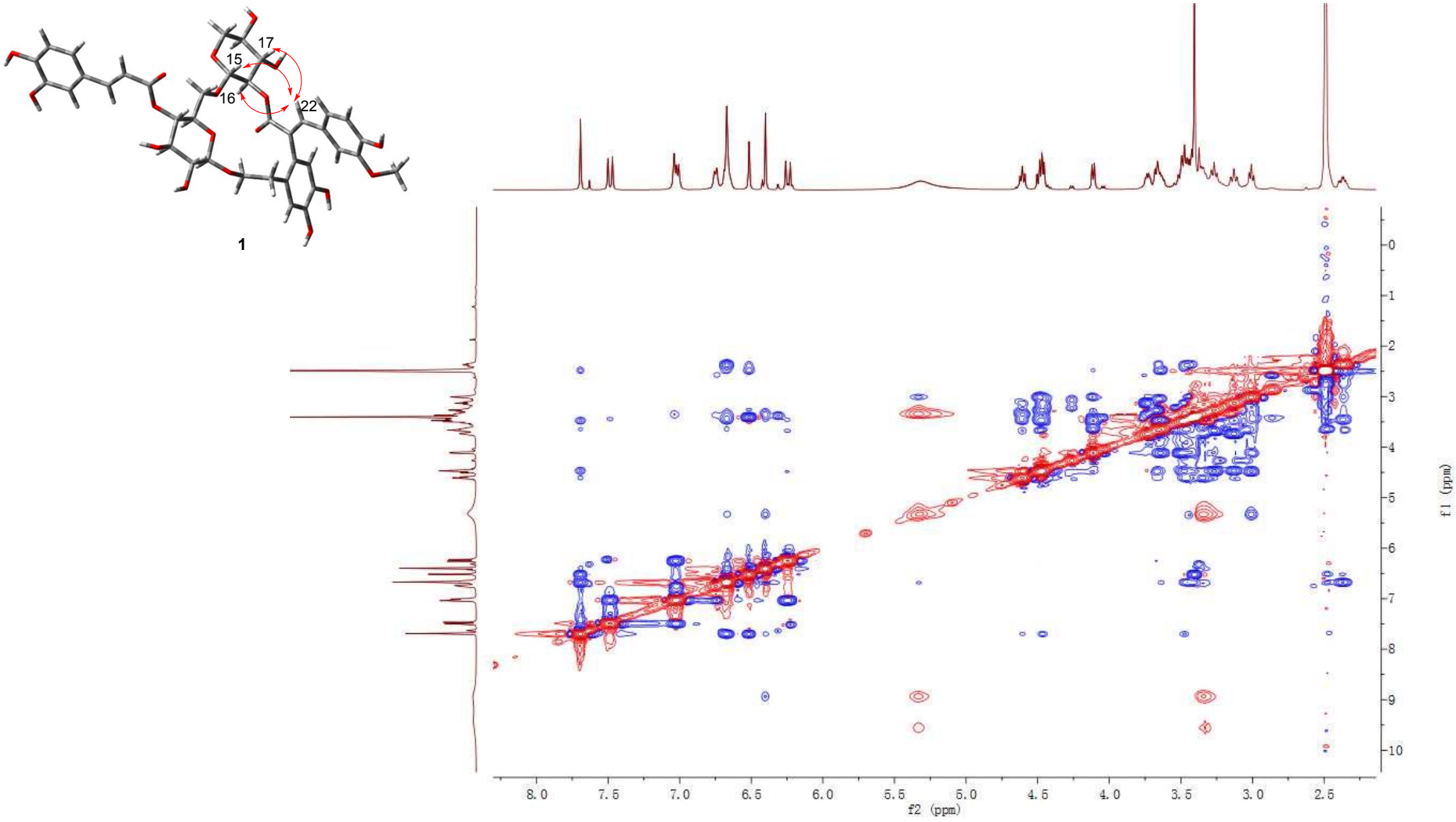

Figure S12. ROESY spectrum of **1** in DMSO-d_6 (500 MHz).

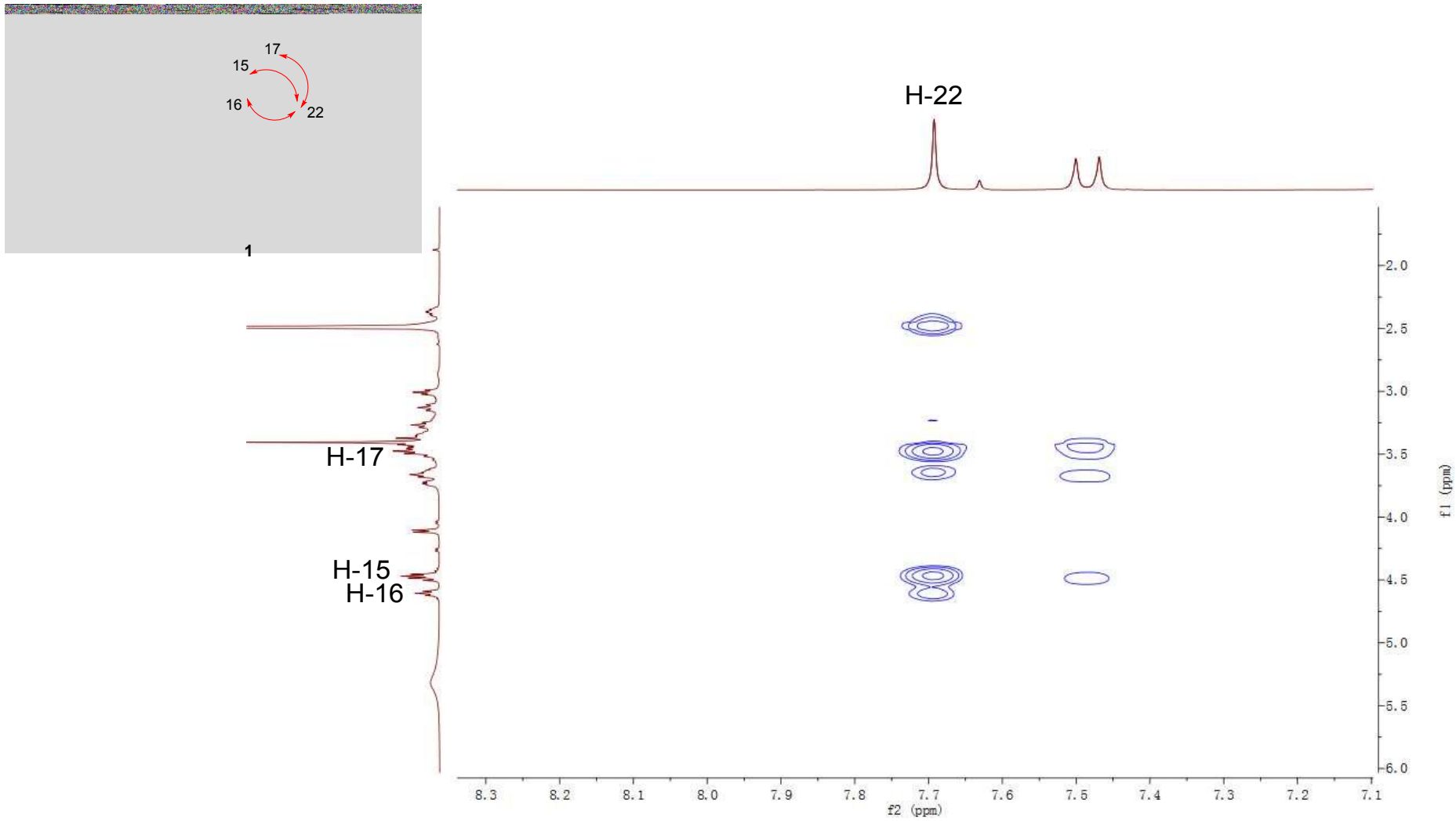

Figure S12a. Expanded ROESY spectrum of **1** in DMSO-d_6 (500 MHz).

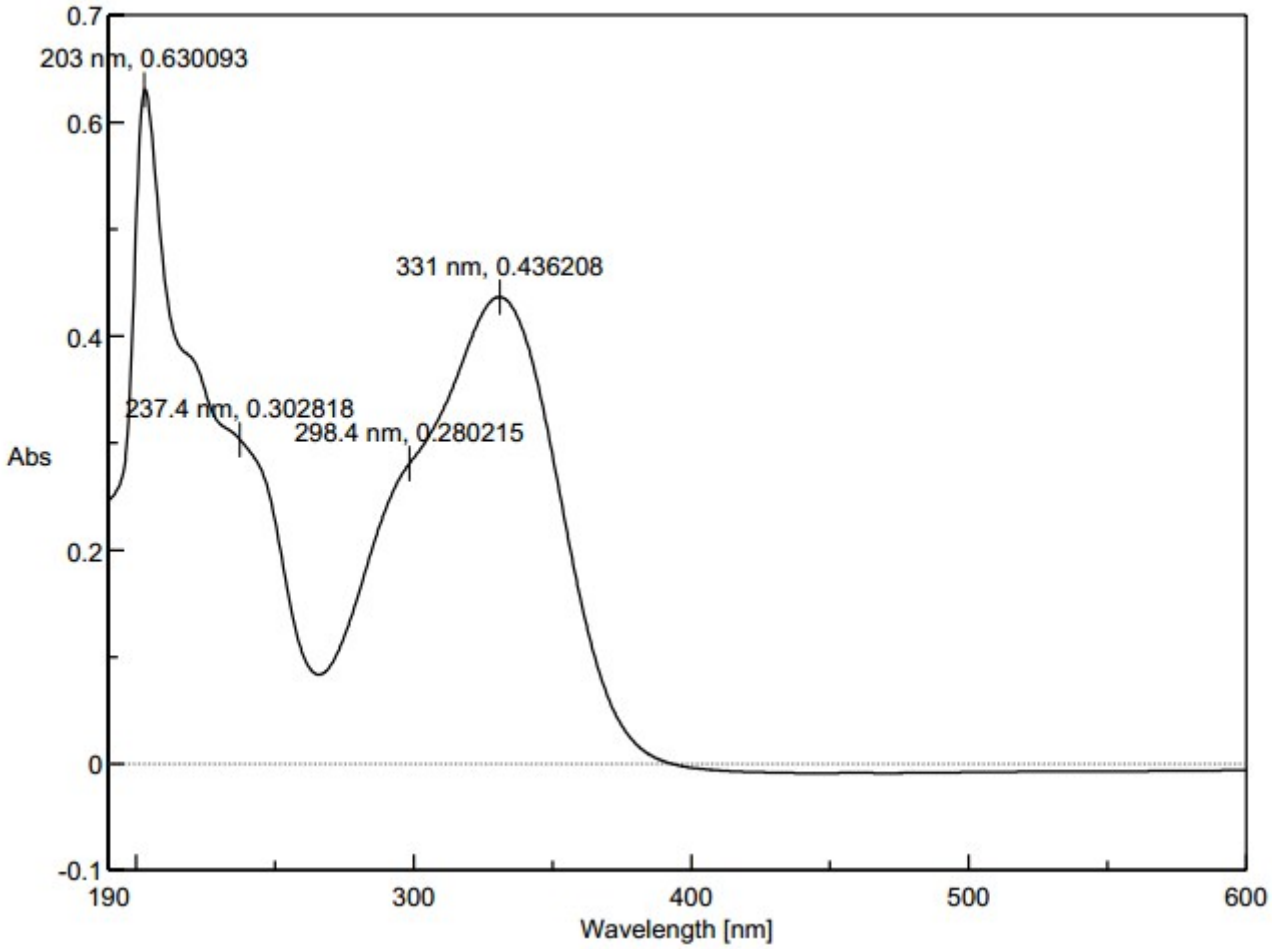

Figure S13. UV spectrum of **2**.

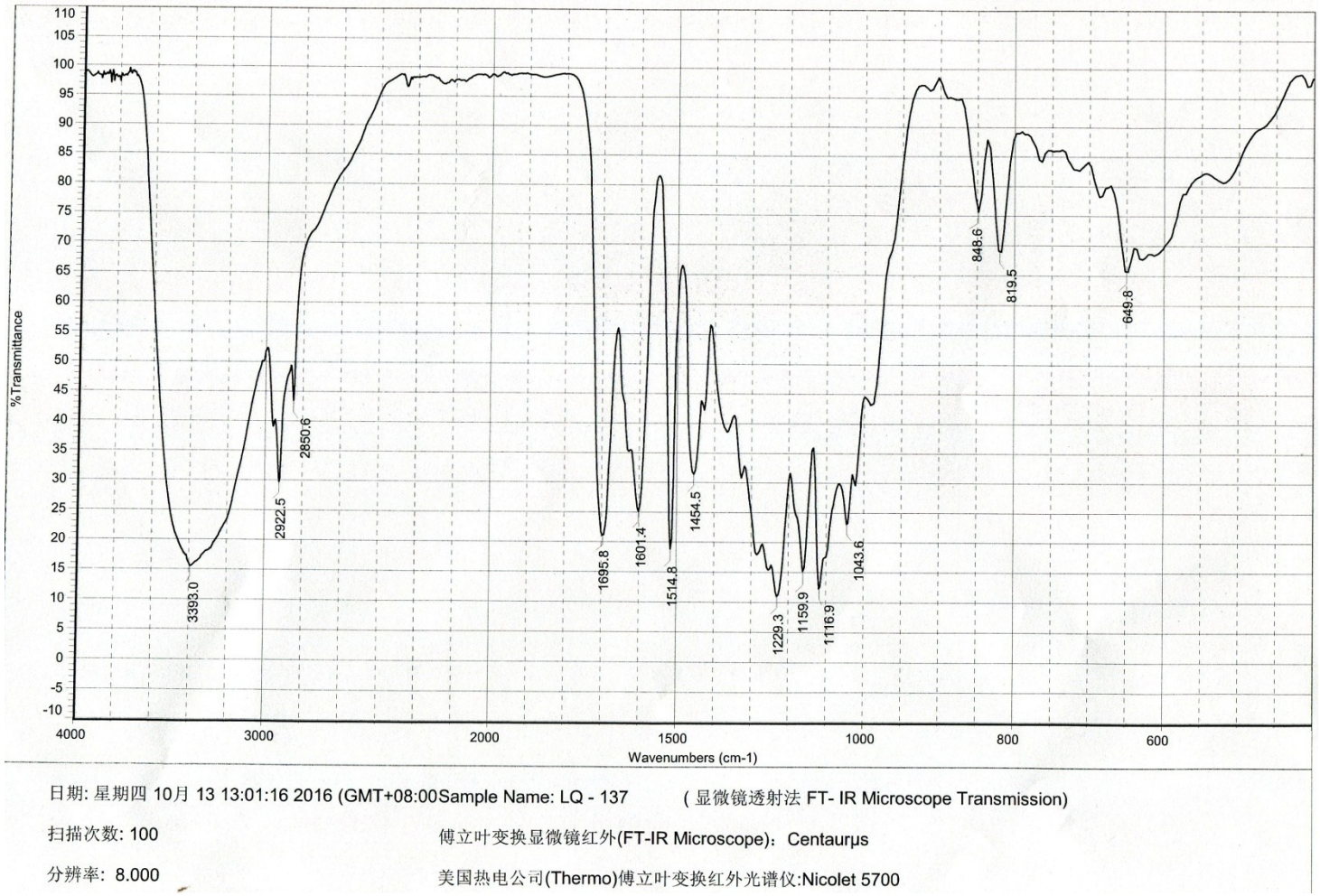

Figure S14. IR spectrum of **2**.

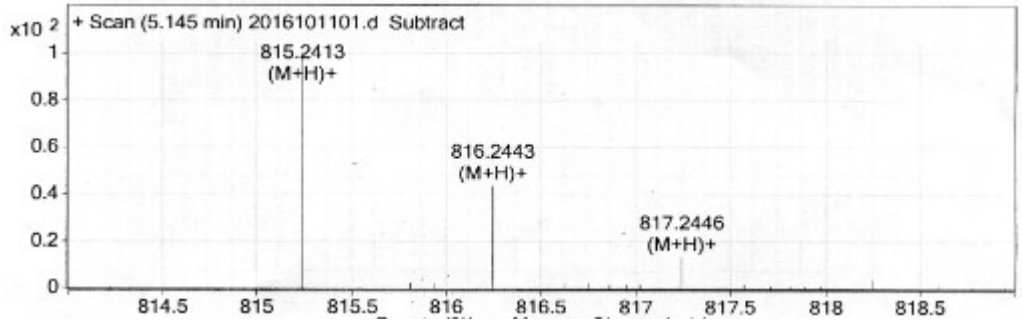

MS Formula Results: + Scan (5.145 min) Sub (2016101101.d)

m/z	Ion	Formula	Abundance
815.2413	(M+H)+	C39 H43 O19	142056.4

Best	Formula (M)	Ion Formula	Score	Cross Sco	Mass	Calc Mass	Calc m/z	Diff (ppm)	Abs Diff (ppm)	Mass Match	Abund Match	Spacing Match	DBE
☑	C39 H42 O19	C39 H43 O19	99.85		814.234	814.232	815.2393	-2.4	2.4	99.79	99.94	99.85	19
☐	C40 H38 N4 O15	C40 H39 N4 O15	99.86		814.234	814.2334	815.2406	-0.78	0.78	99.98	99.67	99.87	24
☐	C37 H42 N4 O15 S	C37 H43 N4 O15 S	99.52		814.234	814.2367	815.244	3.34	3.34	99.6	98.99	100	19
☐	C36 H46 O19 S	C36 H47 O19 S	99.42		814.234	814.2354	815.2427	1.72	1.72	99.89	98.16	100	14
☐	C45 H38 N2 O13	C45 H39 N2 O13	99.17		814.234	814.2374	815.2447	4.17	4.17	99.37	98.27	99.84	28
☐	C44 H38 N4 O10 S	C44 H39 N4 O10 S	99.11		814.234	814.2309	815.2381	-3.87	3.87	99.46	97.78	100	28

Figure S15. HRESIMS of **2**.

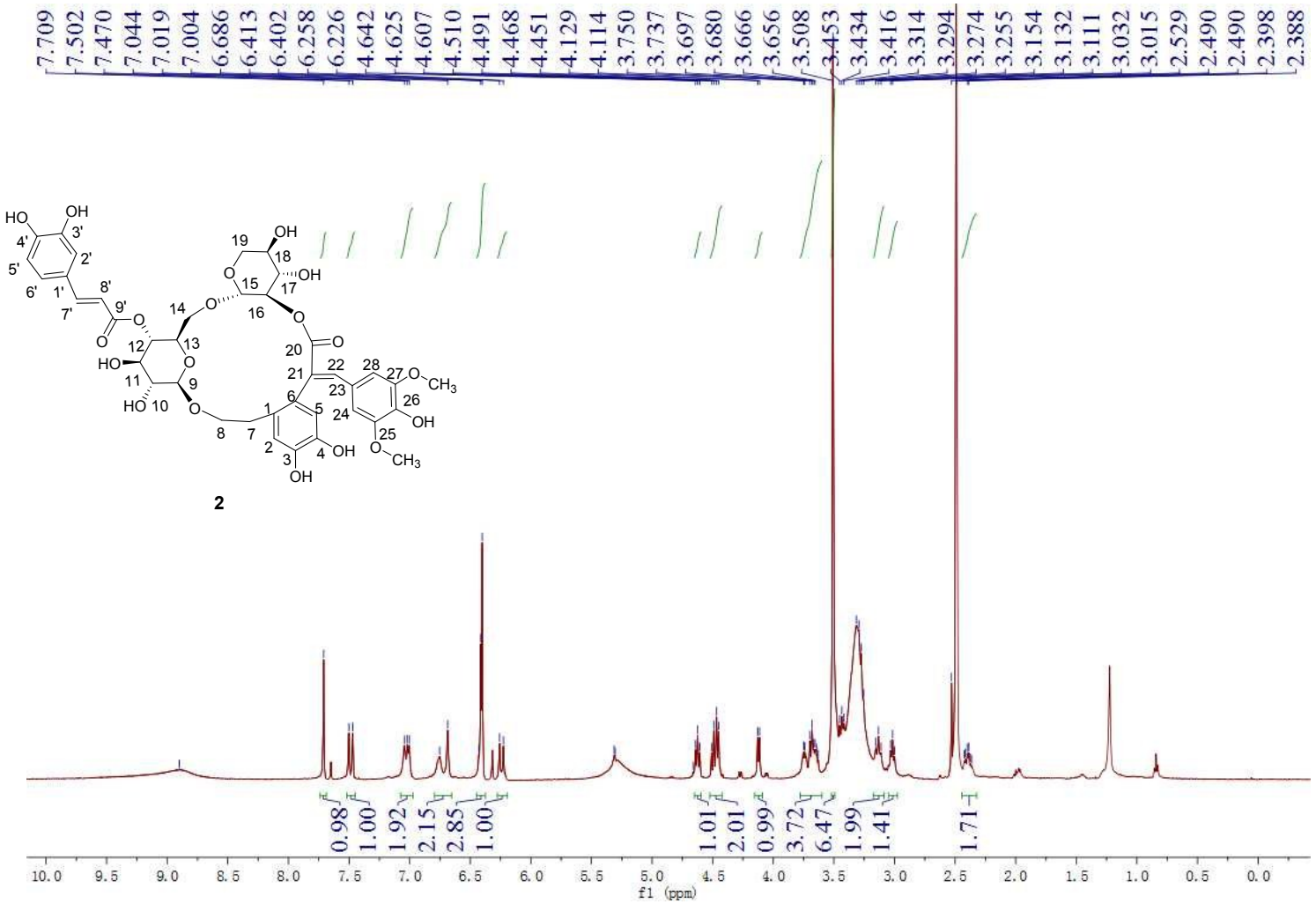

2

Figure S16. ^{1}H NMR spectrum of **2** in DMSO-d_6 (500 MHz).

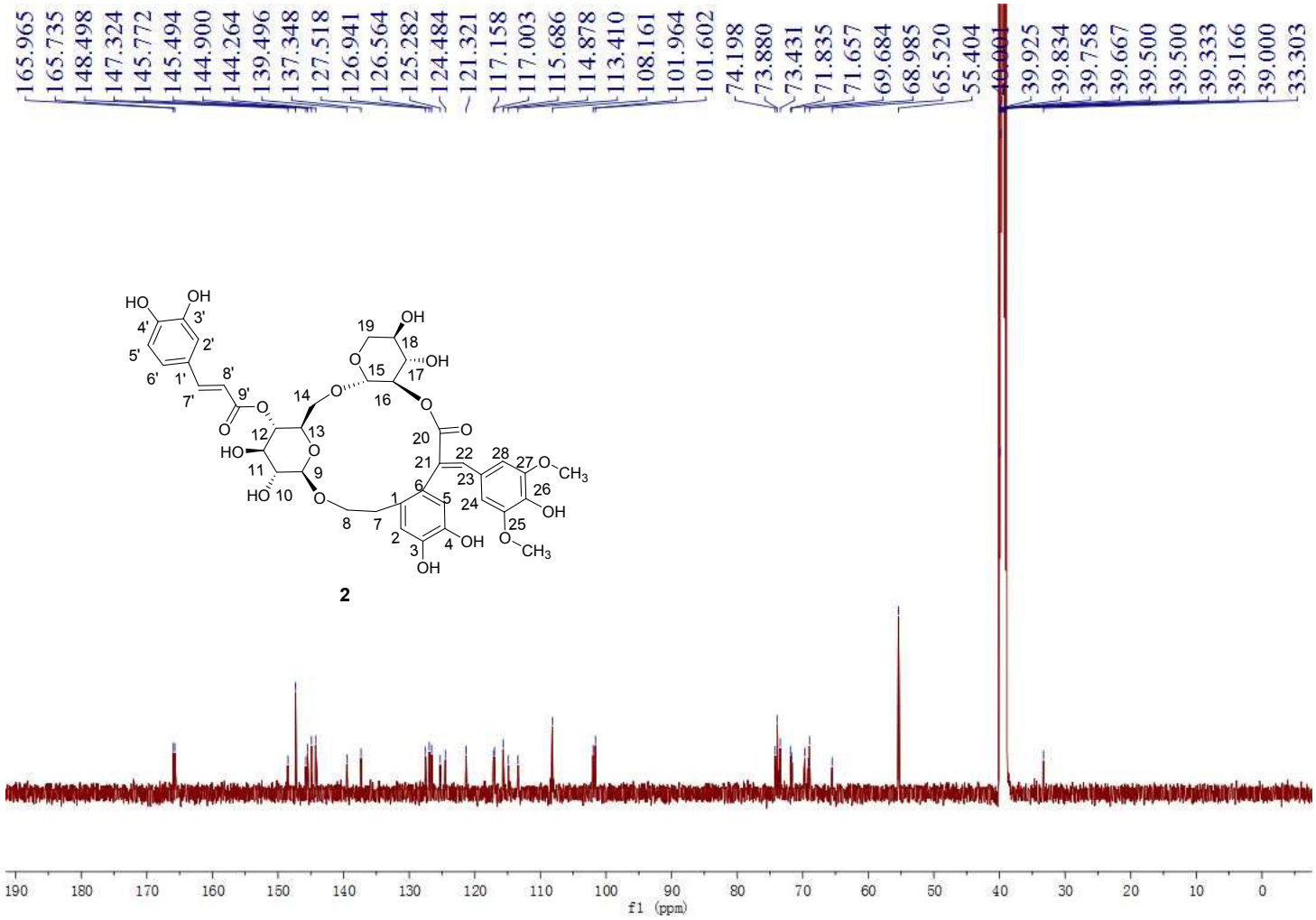

2

Figure S17. ^{13}C NMR spectrum of **2** in DMSO-d_6 (125 MHz)

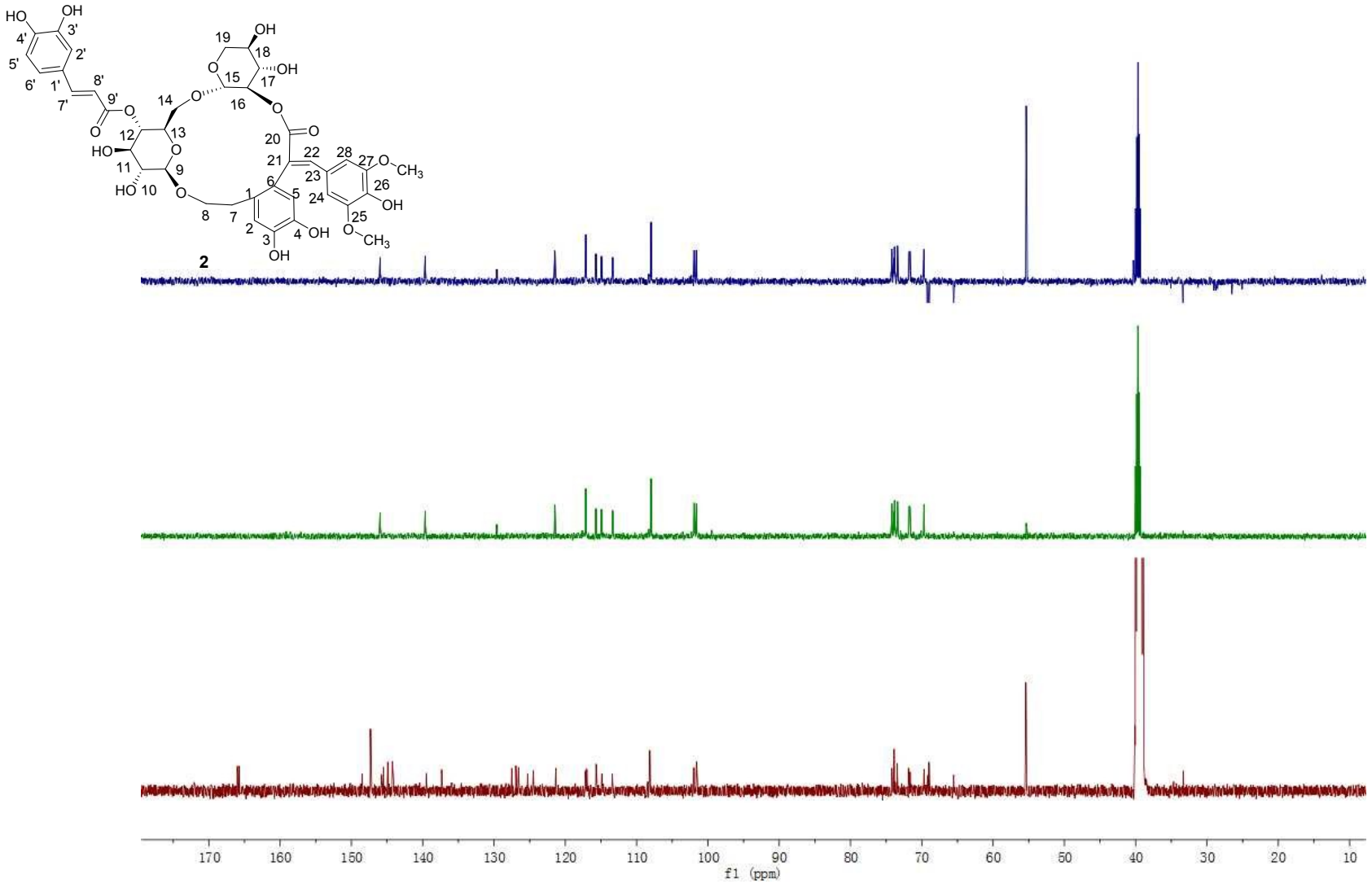

Figure S18. DEPT NMR spectrum of **2** in DMSO-d_6 (125 MHz).

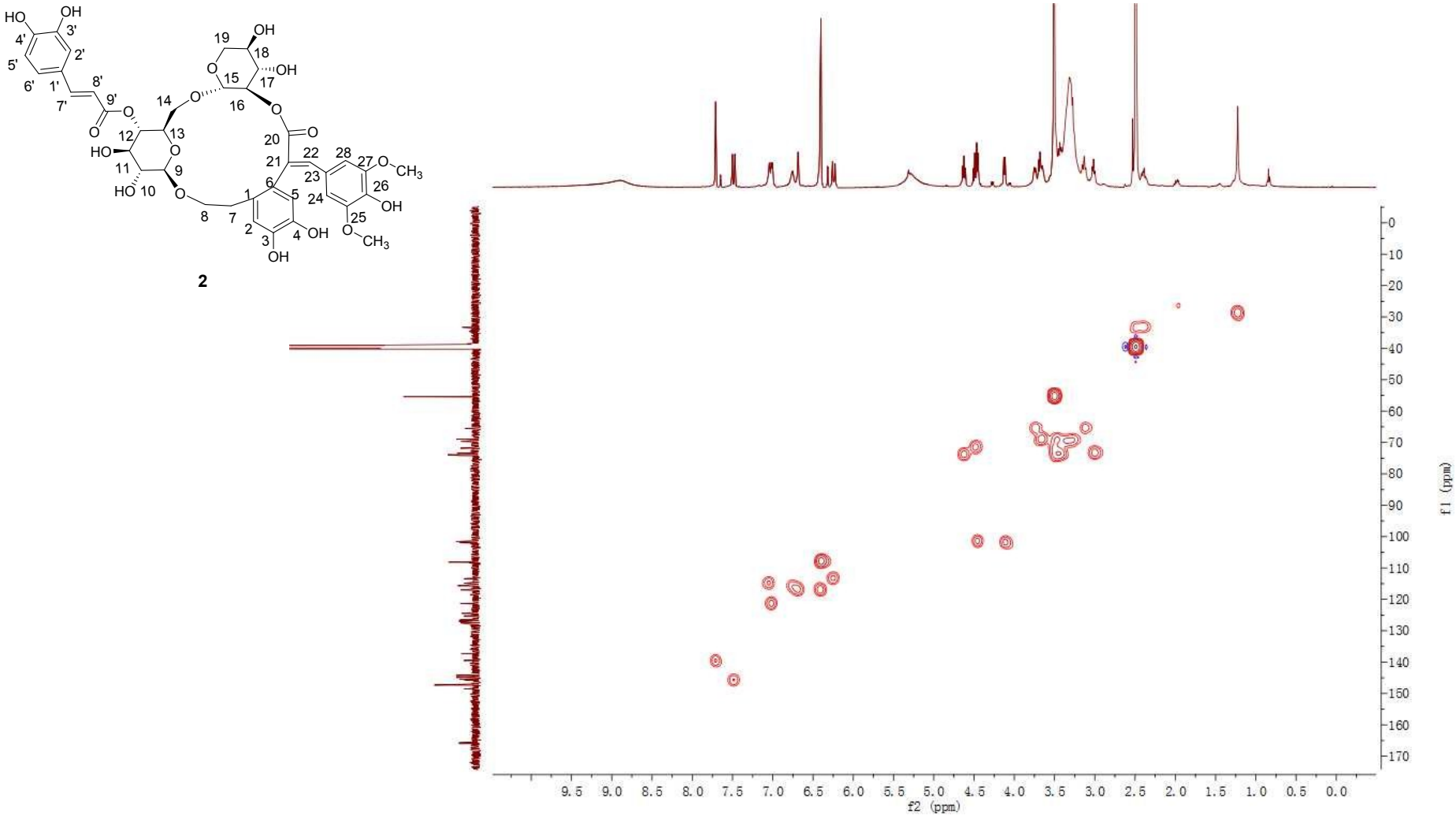

2

Figure S19. HSQC spectrum of **2** in DMSO-d_6 (500 MHz).

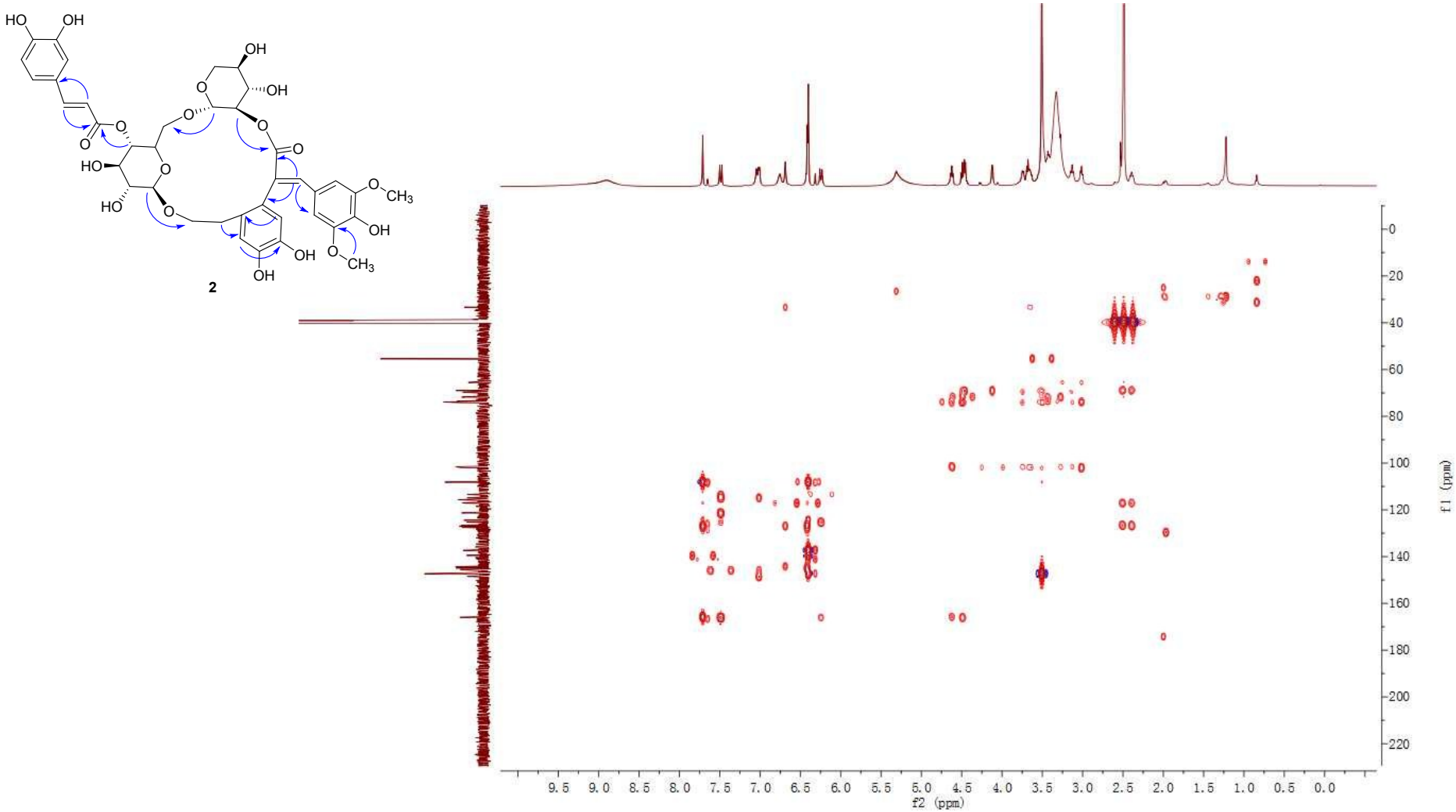

Figure S20. HMBC spectrum of **2** in DMSO-d_6 (500 MHz).

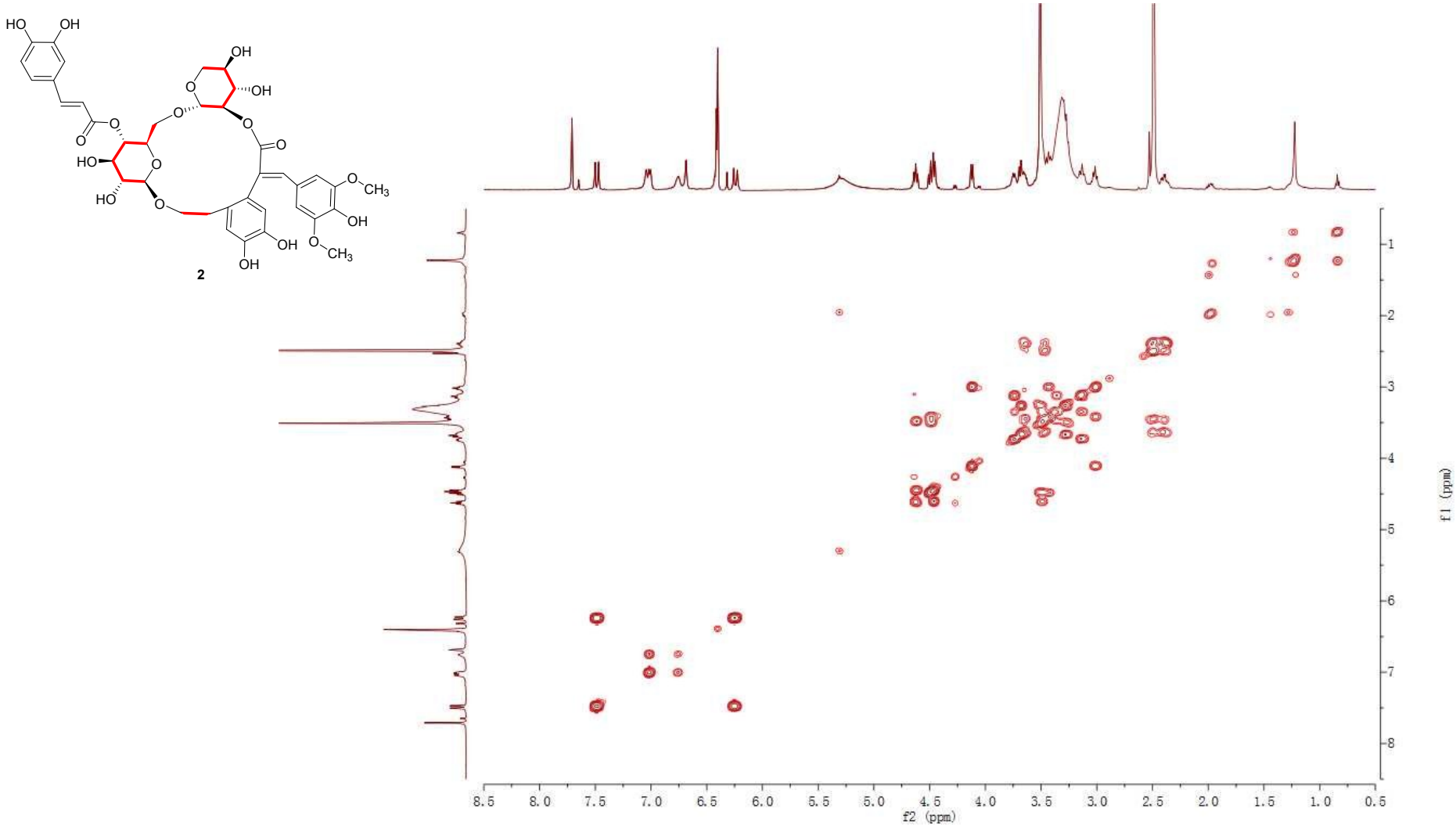

Figure S21. ^{1}H-^{1}H COSY spectrum of **2** in DMSO-d_6 (500 MHz).

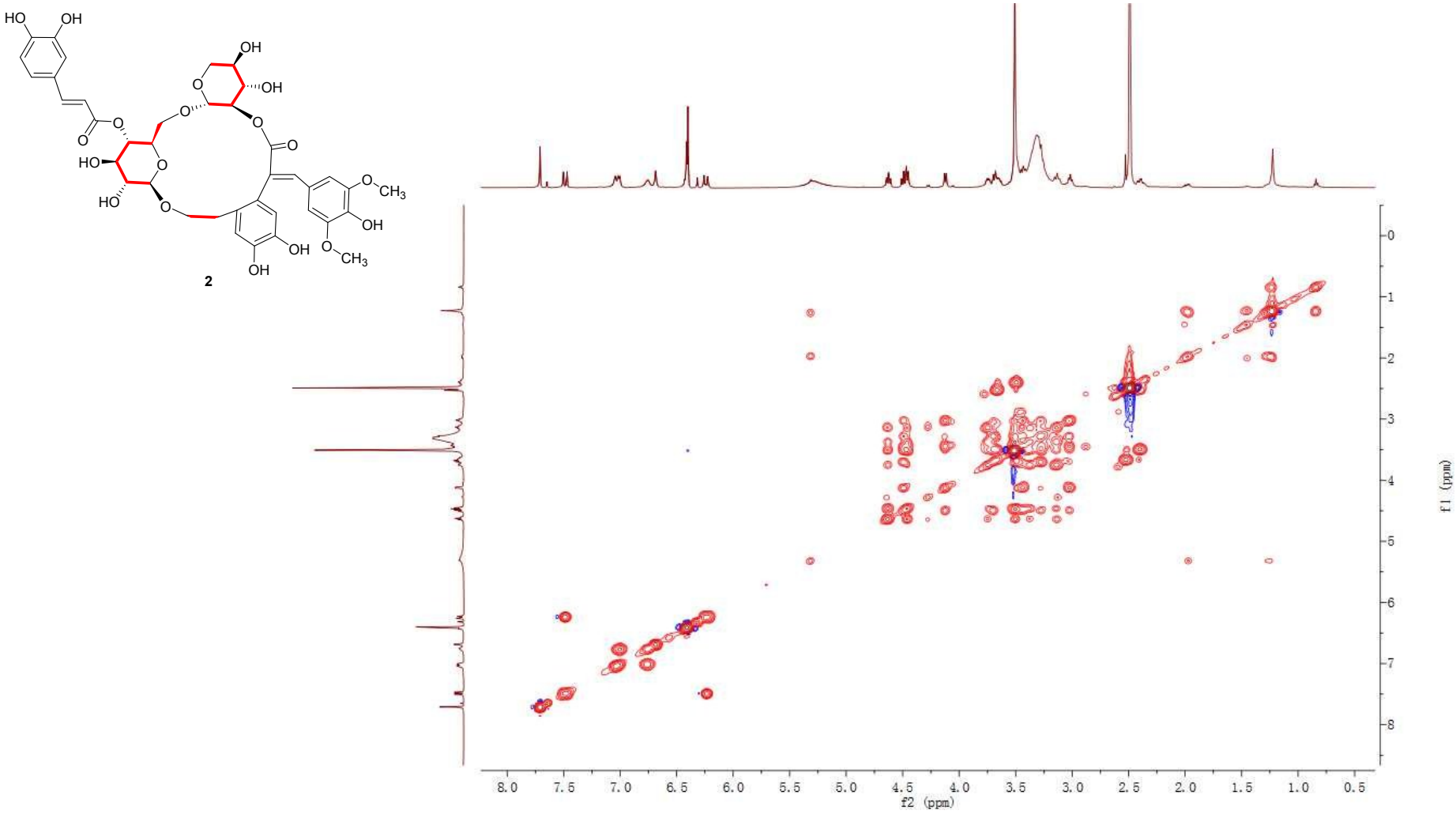

Figure S22. TOCSY spectrum of **2** in DMSO-d_6 (500 MHz).

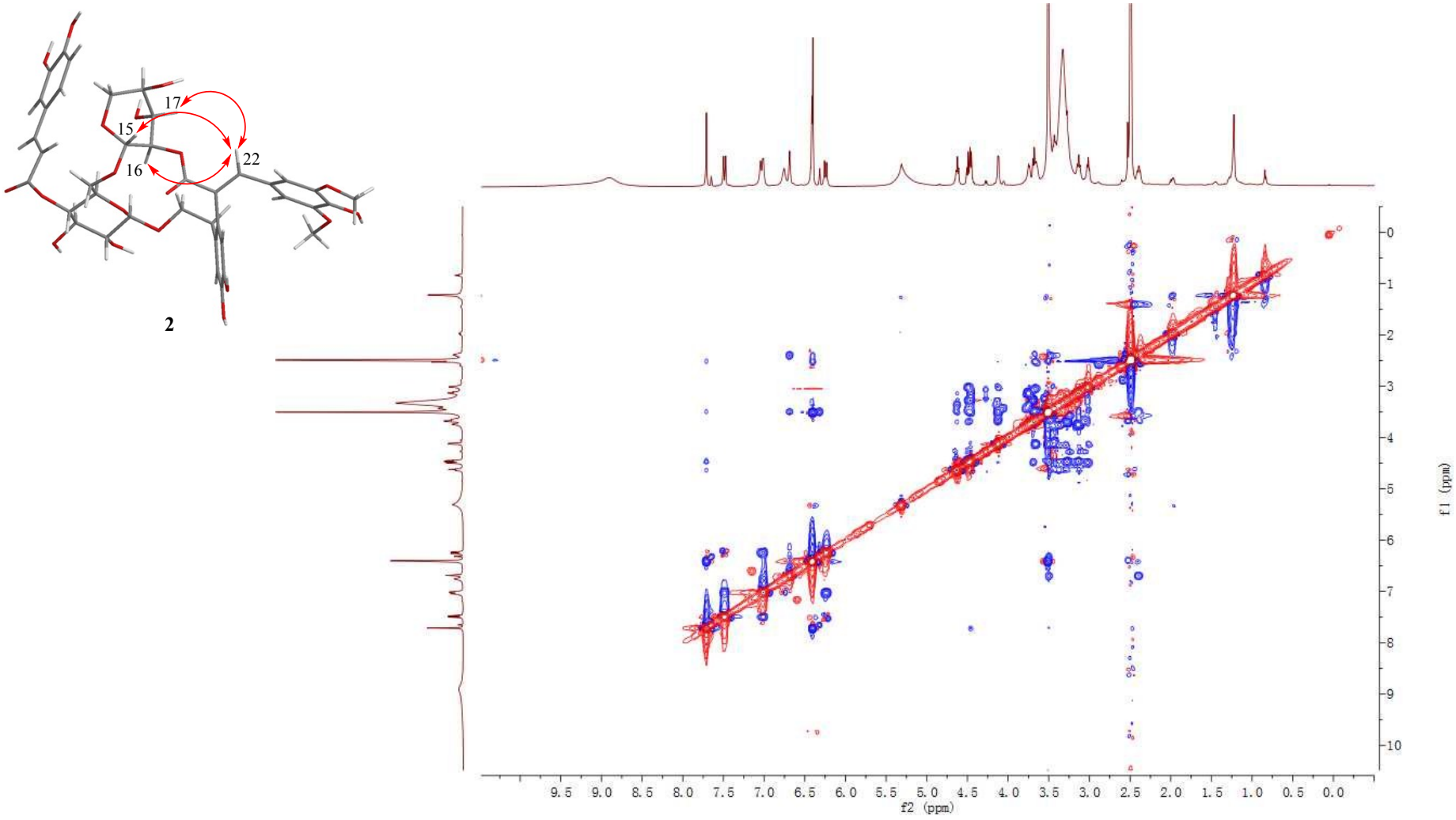

Figure S23. ROESY spectrum of **2** in DMSO-d_6 (500 MHz).

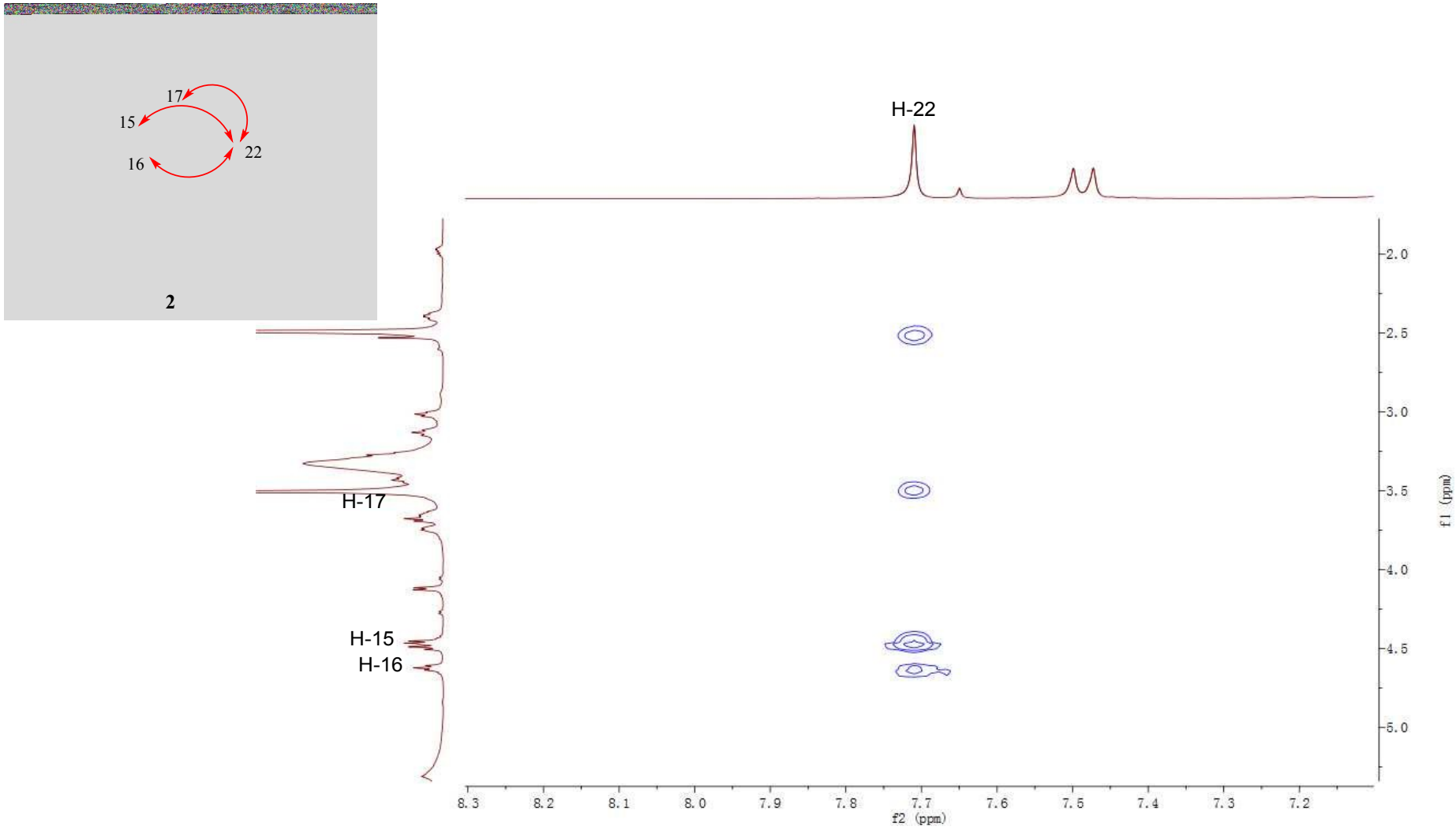

Figure S23a. Expanded ROESY spectrum of **2** in DMSO-d_6 (500 MHz).